

Effect of Acrylonitrile Content of Styrene-co-Acrylonitrile (SAN) on Morphology and Electrooptical Properties of Polymer/Liquid Crystal Composite Films

B. K. KIM* and Y. S. OK

Department of Polymer Science and Engineering, Pusan National University, Pusan 609-735, Korea

SYNOPSIS

Effects of copolymer composition on morphology and electrooptical properties of polymer/liquid crystal (LC) (40/60 w/w) composite films were studied with styrene-co-acrylonitrile (SAN) of varying acrylonitrile (AN) content (6.3–35 wt %) and a cyanobiphenyl-type liquid crystal (E8). The dimension of the LC domain in the composite film decreased with increase of AN content of SAN up to 30 and increased at 35 wt %. The contact angle of the film with an LC drop showed a similar trend; however, its minimum was obtained at 24% AN. Threshold voltage (V_{th}) and rise time (τ_R) increased, and decay time (τ_D) decreased with AN content up to 30%, and the tendency is reversed at 35%. The results were interpreted in terms of, possibly, a solubility parameter matching between SAN and LC. © 1993 John Wiley & Sons, Inc.

INTRODUCTION

Liquid crystals (LCs) have generated considerable interest in regard to use in information displays, where a controllable response of the LC to an applied voltage is made use of.¹ In such a device, LC is sandwiched between conducting glass plates, and this poses restrictions on the device geometry and fabrication of a large-area display.^{1–3}

Polymer/LC composite films have recently been introduced in electrooptical applications.^{3–11} Such composite film is self-supported with mechanical durability and flexibility and with freedom of its geometry for fabrication, especially suitable for large-area displays.^{12–15} Advantages of the composite film over the TN type are well documented in the literature.³ A number of amorphous polymers have been adopted. However, to the knowledge of the present authors, a detailed report on the effect of copolymer composition cannot be found.

This paper describes the use of styrene-co-acrylonitrile (SAN) as a polymer matrix in polymer/LC composite film for optical display. The inter-

actions between polymer and LC molecules should depend on the copolymer composition. SAN of varying acrylonitrile (AN) content (6.3–35 wt %), and a nematic-type liquid crystal (E8) with a positive dielectric anisotropy were used to prepare the film by solvent casting in chloroform. The effect of copolymer composition on morphology and the electrooptical properties of the composite film were studied.

EXPERIMENTAL

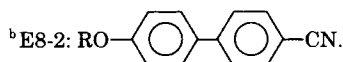
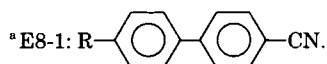
Basic molecular parameters of SAN are given in Table I. E8 is a mixture of nematic liquid crystal (cyanobiphenyl derivatives, BDH Chemical) with $T_{KN} = 261$ K (crystal-to-nematic transition temperature), $T_{NI} = 345$ K (nematic-to-isotropic transition temperature), n_e (extraordinary refractive index) = 1.774, n_o (ordinary refractive index) = 1.527, and η (viscosity) = 54 cPs at 298 K with positive dielectric anisotropy. The film was prepared by the solvent-induced phase separation (SIPS) method in chloroform at room temperature.³ The thickness of the film was 30 ± 0.5 μm . To study the morphology of the film, LC domains were first extracted in methanol for 10 h, and films were frac-

* To whom correspondence should be addressed.

Table I Molecular Weight of SAN, Solubility Parameter of SAN and E8, and Major Domain Size of LC in Composite Films

	SAN						E8	
	AN Content (wt %)						E8-1 ^a	E8-2 ^b
	6.3	11	14.7	24	30	35		
Molecular weight (MW)	343,000	198,000	181,000	124,000	160,000	145,000		
Solubility parameter (δ) (cal/cm ³) ^{1/2}	8.777	8.940	9.070	9.401	9.617	9.799	9.53–9.58	9.36–9.47
Major domain size (μ m)	1.6	1.45	1.4	1.2	1.02	1.15		
Maker	Dow	Asahi	Asahi	Lucky	Dow	Hyosung	BDH	

R: alkyl chain containing 1–12 carbon atoms.



tured at liquid N₂ temperature, followed by sputtering with gold before viewing under a scanning electron microscopy (SEM, JEOL JSM-820). The average dimension of the LC domain was determined from the SEM micrographs. For this, a few parallel straight lines were drawn on the micrographs, and holes on the lines were identified with their major dimension. Usually, 30 holes were measured on average.

For electrooptical measurements, the film, across which an electric field was applied, was first sandwiched between two indium–tin oxide (ITO)-coated glass plates. A laser (He–Ne, wavelength 632.8 nm) beam was incident normal to the film surface and the transmittance through the film was recorded using a digital storage oscilloscope (Hitachi, VC-6023). The distance between cell and photodiode was 305 mm. The contact angle of the film surface with water and E8 drops was measured using a contact angle meter (Erma) at room temperature.

RESULTS

Film Morphology

Figure 1 shows the SEM micrographs of the fractured surface of polymer/LC (40/60 w/w) composite film. It is seen that both SAN (white region) of spongelike network and LC domains (dark region) are continuous. The structural heterogeneity is a source of optical heterogeneity for the composite

in the absence of an external field. It is seen that the LC domain becomes larger as the AN content of SAN increases up to 30% and becomes smaller at 35% AN. The number-average major dimension of the dispersed domains, measured from the SEM micrographs, is also given in Table I. Generally, in immiscible polymer blends and composites, reduction of the dispersed domain occurs when the interactions between the two phases increase.^{16–18}

In the absence of an external field, the LC molecule will adopt a configuration of minimum free energy of the LC domain, which is determined by the interaction at the polymer–LC interface.¹⁹ In most polymer/LC composite films, the optic axis of LC molecules varies randomly from domain to domain in the absence of an external field. Upon applying the electric field across the film, the LC molecules will tend to align with their nematic director along the applied field (positive dielectric anisotropy). At this time, a much stronger external field should be applied when the polymer–LC interactions are strong. In this regard, it is expected that smaller LC domains would require a stronger electric field to orient the LC molecules along the field direction.

Voltage Dependence of Transmittance and Response Times

Transmittance as a function of voltage at 1 kHz is shown in Figure 2. It is clearly seen that the thresh-

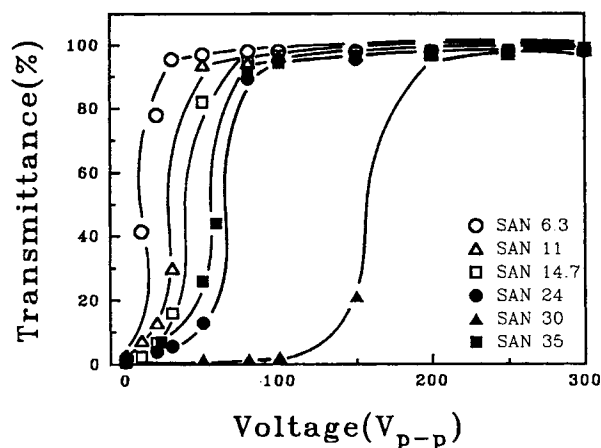


Figure 2 Transmittance vs. applied voltage (1 kHz, 300 K).

old voltage (V_{th}), i.e., the voltage at which the transmittance becomes 10%, and the breadth of the threshold ($V_{10} - V_{90}$) strongly depend on the composition of the polymer matrix. V_{th} is less than $10 V_{p-p}$ for SAN containing 6.3% AN and it increases with AN content of SAN up to 30%, where a maximum ($> 130 V_{p-p}$) is obtained. V_{th} decreases below $30 V_{p-p}$ at 35% AN. In polymer-dispersed LC, the threshold voltage is approximated by the following equation²⁰:

$$V_{th} = \frac{d}{R} \left[\frac{K(l^2 - 1)}{\epsilon_0 \Delta \epsilon} \right]^{1/2} \quad (1)$$

where d is the film thickness, R , the droplet radius; K , the effective elastic constant; $\Delta \epsilon$, the dielectric anisotropy; ϵ_0 , the vacuum dielectric constant; and l , the aspect ratio of the LC droplet (major dimension/minor dimension). This equation states that V_{th} does not directly depend on the matrix characteristics. Instead, the effect of matrix, i.e., the interaction between the matrix and the LC, is introduced via the dispersed domain size [R in eq. (1)]. The dependence of V_{th} on AN content is opposite to the LC domain size and the present results qualitatively agreed with eq. (1). The variation of transmittance with voltage is due to the LC domain alignment along the electric field.²¹ As the domain size of the LC decreases, interfacial areas between the polymer and the LC increase, and a stronger electric field becomes necessary to overcome the interfacial interactions.

Rise time (τ_R) and decay time (τ_D) as a function of voltage are shown in Figures 3 and 4. τ_R is conventionally defined as the time for a transmittance change from 10 to 90% upon turning the electricity

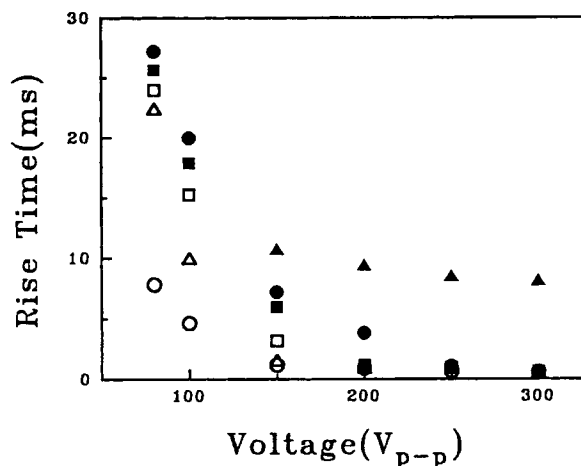


Figure 3 Rise time vs. applied voltage (1 kHz, 300 K; same as Fig. 2).

on, and τ_D , as the reverse of τ_R , measured upon turning the electricity off. It is seen that τ_R increases with AN up to 30% and decreases at 35%. The variation of τ_D with voltage is generally much smaller when compared with τ_R , and this is probably due to the residual electric charge in the measuring cell serving as a capacitor.¹ However, it is clear that the decay time decreases with AN content up to 30% and slightly increases at 35% AN, and the tendency is exactly opposite to the rise time. Rise time is calculated by balancing electric, elastic, and viscous torque densities, with the following result²²:

$$\tau_R^{-1} = \frac{1}{\eta} \frac{9\epsilon_0 \Delta \epsilon V^2}{d^2 (\rho_p / \rho_{LC} + 2)^2} + \frac{K(l^2 - 1)}{\eta a^2} \quad (2)$$

In the above equation, η is the viscosity; ρ , the re-

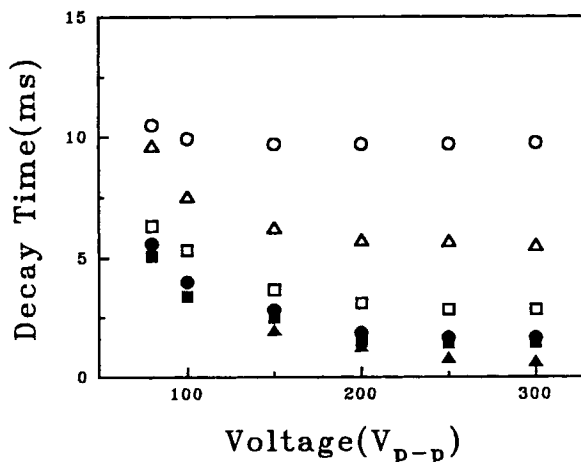


Figure 4 Decay time vs. applied voltage (1 kHz, 300 K; same as Fig. 2).

sistivity; and a , the major dimension of the dispersed domain; subscripts p and LC designate polymer and liquid crystal, respectively, and other symbols are the same as in eq. (1). Decay time is simply obtained by letting $V = 0$ in eq. (2). Since τ_R is normally dominated by the first term, the effect of domain size does not directly enter the equation. The variation of τ_D with copolymer composition follows that of the dispersed domain size (a) and qualitatively agrees with eq. (2) ($\tau_R \rightarrow \tau_D, V = 0$).

Frequency Dependence of Response Times

Variation of response times with frequency (Figs. 5 and 6) shows a similar tendency to that of voltage. However, it is noted that the frequency dependence of τ_R and τ_D is, respectively, smaller and larger than the voltage dependence. The optical response of the composite to electric frequency should come from the partition of the external electric field (E) to the polymer (E_p) and LC (E_{LC}) domains,³ i.e., E_p/E and E_{LC}/E . For example, in a composite composed of polymer and LC in a series, the ratio of E_p to E_{LC} can be written as^{23,24}

$$\begin{aligned} E_{LC}/E_p &= \epsilon_p^*/\epsilon_{LC}^* \\ &= \{(\omega^2\epsilon_p'^2 + \sigma_p^2)/(\omega^2\epsilon_{LC}'^2 + \sigma_{LC}^2)\}^{1/2} \quad (3) \end{aligned}$$

where E is the amplitude of external electric field; ϵ^* , the complex dielectric constant; ϵ' , the in-phase component of the dielectric constant; ω , the angular frequency; and σ , the conductivity. The equation states that at high enough frequencies (the case en-

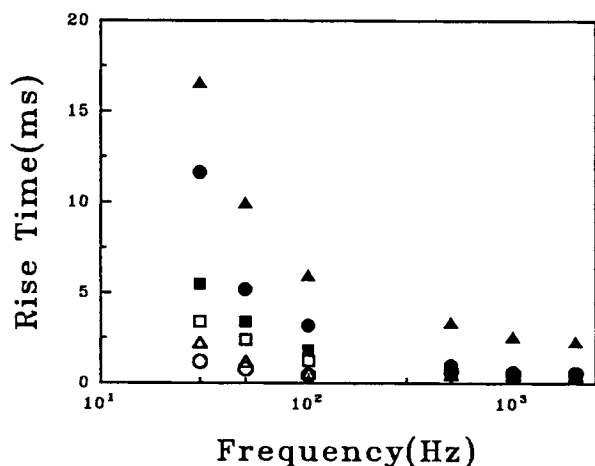


Figure 5 Rise time vs. applied frequency (250 V_{p-p} , 300 K; same as Fig. 2).

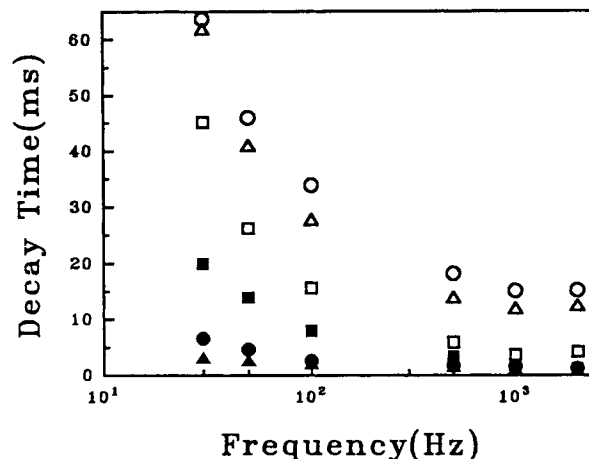


Figure 6 Decay time vs. applied frequency (250 V_{p-p} , 300 K; same as Fig. 2).

countered here), the ratio is inversely proportional to the dielectric constant ratio. To take this into consideration, ϵ of SAN was calculated from the group contribution.²³ ϵ increases monotonically with the AN of SAN (2.58 for 6.3 and 2.73 for 35% AN). With the increase of ϵ_p , higher E_{LC} results and a smaller rise time is expected due to greater partition of the external field on LC domains. However, the results of Figure 5 do not confirm this, and it is, rather, the opposite.

On the other hand, for composites with different dielectric properties, the external field will induce interfacial polarizations and augments E_{LC} . During the process of interfacial polarization, partition of E to E_{LC} would increase.²² The interfacial polarization should increase with the increase of the interfacial area, i.e., SAN of 30% AN, which has smallest LC domain, is supposed to give minimum τ_R since it induces maximum interfacial polarization and the highest partition of E to E_{LC} . However, this effect does not show up, either. This may, in part, be due to the contamination of each phase with the other, lowering the resistivity of both phases.²²

It seems that the key property to control the response time as well as other electrooptical properties is the morphology of the composite, i.e., the domain size of LC in SAN, which agrees with the electrooptical response. Perhaps, the contribution of electric field partition to the LC phase is of one order of magnitude higher than that of the LC domain size. This postulation can possibly be seen from Figure 5, i.e., the composite films having relatively large LC domains give a practically insignificant difference in τ_R among themselves and show little change in frequency as well.

Contact Angle

Figure 7 shows the contact angle of the film with E8 and water. For this purpose, the film was prepared from solvent cast of SAN in chloroform, and, hence, the film contains neither LC nor vacancy. The variation of contact angle with AN of SAN shows a similar trend for E8 and water. Since the films do not contain the LC domain or vacancy in it, the variation of the contact angle is a purely polymer effect. It is also clear that the contact angle of water (75–94.2°) is significantly greater than that of E8 (12.4–34.8°) and the AN content of the minimum contact angle (30% AN) is higher than that of E8 (24%). These differences should come mainly from the difference in the chemical affinity of E8 and water toward the film and should have same origin with the morphology variation along with copolymer composition.

DISCUSSION

The variations of electrooptical response and contact angle with copolymer composition seems to follow the morphology of the composites. Also, since the morphology is governed mainly by the chemical affinity between the components, we calculated the solubility parameters (δ) of SAN and E8 (Table I). E8 is a mixture of cyanobiphenyl derivatives, and the length of the alkyl chain is in the range of 1–12 carbon atoms. Assuming E8 is a 50/50 mixture of the two types of LC (see Table I), and each alkyl

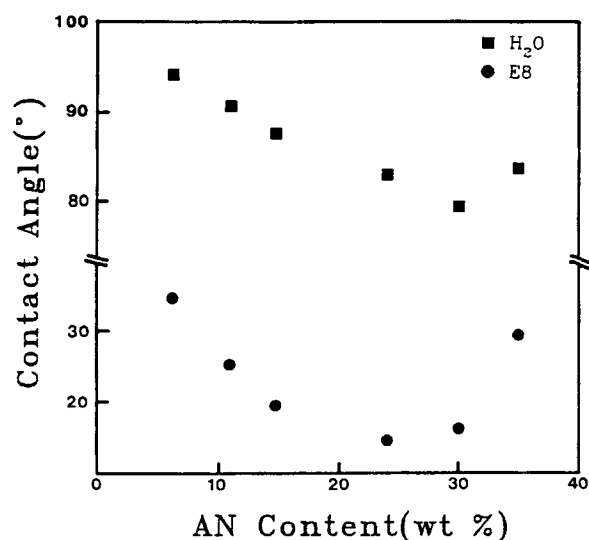


Figure 7 Contact angle vs. AN content of SAN at room temperature.

group contains 5 carbon atoms, δ of E8 is about 9.48 (cal/cm^3)^{1/2}. It is seen that the solubility parameter of SAN nears that of E8 when the AN content of SAN is 24%, and the result agrees well with the measured contact angle. This indicates that the key parameter controlling the film properties is the solubility parameter, and the best chemical affinity between SAN and E8 is obtained at this copolymer composition. Much greater contact angle and shift of minimum to higher AN for water is due mainly to the much higher solubility parameter of water [ca. 23.4 (cal/cm^3)^{1/2}] over the E8 and SAN. (Note that δ of SAN monotonically increases with AN.)

The AN content of SAN (24%) where minimum contact angle and solubility parameter matching were obtained does not exactly match with the content for minimum LC domain size and highest V_{th} (30%). This may be due, in part, to the connectivity of the LC domains, i.e., polymer and LC phases are cocontinuous in our film, and correct identification of LC domain size is not possible. However, this disagreement may imply that chemical affinity between polymer and LC does not solely govern the morphology and electrooptical response of the film. The intramolecular repulsion of SAN could be considered as follows:

A certain random copolymer of monomers A and B is miscible with homopolymer C in a certain range of copolymer composition (miscibility window), whereas homopolymer C is not miscible with homopolymer A or B.²⁵ Such a phenomenon is properly explained in terms of the concept that the repulsions between the units within copolymer may promote their miscibility. SAN is a typical copolymer that shows a miscibility window with a number of homopolymers. For example, SAN/PMMA [poly(methyl methacrylate)] blends show an LCST (lower critical solution temperature) when the AN content of SAN is in the range of 9–28 wt %.^{25–27} Since the miscibility of a copolymer with a homopolymer is driven by the intrachain repulsions of the copolymer, a similar effect is expected between SAN and low molar mass LC. The relatively smaller LC domain size is up to 30, and the larger one at 35% AN in SAN apparently resembles the phase behavior of SAN/PMMA blends.

The variation of V_{th} with AN of SAN may primarily come from the LC domain size. With smaller dimensions of LC domains, more LC molecules interact with the polymer wall and a stronger external field is necessary to overcome the polymer–LC interfacial interactions and to align themselves along the electric field. This should provide the composite with higher V_{th} and τ_R . On the contrary, upon turn-

ing the field off, randomization of the nematic directors becomes easier when the interfacial interactions are stronger, which would give smaller τ_D .

The support of Korean Science and Engineering Foundation (Grant No. P21-0600-004-2) is gratefully acknowledged.

REFERENCES

1. E. B. Priestley, P. J. Wojtowicz, and P. Sheng, *Introduction to Liquid Crystals*, Plenum Press, New York, 1974.
2. N. March and M. Tosi, *Polymers, Liquid Crystals, and Low-Dimensional Solids*, Plenum Press, New York, 1984.
3. A. Miyamoto, H. Kikuchi, Y. Morimura, and T. Kajiyama, *New Polym. Mater.*, **2**, 1 (1990).
4. D. Dutta, H. Fruitwala, A. Kohli, and R. A. Weiss, *Polym. Eng. Sci.*, **30**, 1005 (1990).
5. P. Drazic and K. Werner, *Infor. Display*, **2**, 6 (1989).
6. W. D. McIntyre and D. S. Soane, *Am. Chem. Soc. Div. Polym. Chem. Polym. Prepr.*, **29**, 197 (1988).
7. N. A. Vaz and G. Paul Montgomery, Jr., *J. Appl. Phys.*, **62**(8), 3161 (1987).
8. P. S. Drazalic, *J. Appl. Phys.*, **60**(6), 2142 (1986).
9. J. L. Ferguson, U.S. Pat. 4,616,903 (1986).
10. J. L. Ferguson, U.S. Pat. 4,435,047 (1984).
11. J. W. Doane, N. A. Vaz, B. G. Wu, and S. Zumer, *Appl. Phys. Lett.*, **48**, 269 (1986).
12. T. Kajiyama, Y. Nagata, S. Washizu, and M. Takayanagi, *J. Membr. Sci.*, **11**, 39 (1982).
13. T. Kajiyama, S. Washizu, and M. Takayanagi, *J. Appl. Polym. Sci.*, **29**, 3955 (1984).
14. T. Kajiyama, S. Washizu, A. Kumano, I. Terada, M. Takayanagi, and S. Shinkai, *J. Appl. Polym. Sci. Appl. Polym. Symp.*, **41**, 327 (1985).
15. T. Kajiyama, H. Kikuchi, A. Miyamoto, S. Moritomi, and J. C. Hwang, *Chem. Lett. (Jpn. Soc. Chem.)*, 817 (1989).
16. P. R. Hornsby, in *Two-Phase Polymer System*, L. A. Utracki, Ed., Oxford University Press, New York, 1991.
17. C. D. Han, *Multiphase Flow in Polymer Processing*, Academic Press, New York, 1981.
18. B. K. Kim, S. Y. Park, and S. J. Park, *Eur. Polym. J.*, **27**, 349 (1991).
19. G. P. Montgomery, *SPIE Instit. Ser.*, **1S 4**, 577 (1990).
20. J. W. Doane, A. Golemme, J. L. West, J. B. Whiteheat, Jr., and B. G. Wu, *Mol. Cryst. Liq. Cryst.*, **165**, 511 (1988).
21. L. L. Chapoy, *Recent Advances in Liquid Crystalline Polymers*, Elsevier, New York, 1986.
22. J. W. Doane, in *Liquid Crystals-Applications and Uses*, B. Bahadur, Ed., World Scientific, Singapore, 1990, Vol. 1.
23. D. W. Van Krevelen and P. J. Hoftyzer, *Properties of Polymer*, Elsevier, New York, 1980.
24. T. Kajiyama, H. Kikuchi, and A. Miyamoto, *Chem. Lett. (Jpn. Soc. Chem.)*, **4**, 434 (1990).
25. M. Nishimoto, H. Keskkula, and D. R. Paul, *Polymer*, **30**, 1279 (1989).
26. J. Lyngaae-Jorgensen and K. Sondergaard, *Polym. Eng. Sci.*, **27**, 351 (1987).
27. J. Kressler, H. W. Kammer, and K. Klostermann, *Polym. Bull.*, **15**, 113 (1986).

Received October 13, 1992

Accepted January 8, 1993